

Modelling and Numerical Simulation of Nonclassical Effects of Waves, including Phase Transition Fronts

Arkadi Berezovski,^{1,3} Jüri Engelbrecht,¹ and Gerard A.Maugin²

Short title: Modelling and Numerical Simulation

¹ Centre for Nonlinear Studies, Institute of Cybernetics at Tallinn University of Technology, Akadeemia tee 21, 12618 Tallinn, Estonia

² Laboratoire de Modélisation en Mécanique, Université Pierre et Marie Curie, UMR 7607, Tour 65-55, 4 Place Jussieu, Case 162, 75252, Paris Cédex 05, France

³ To whom correspondence should be addressed. Arkadi Berezovski, Centre for Nonlinear Studies, Institute of Cybernetics at Tallinn University of Technology, Akadeemia tee 21, 12618 Tallinn, Estonia; e-mail: Arkadi.Berezovski@cs.ioc.ee

Abstract—A thermodynamically consistent finite-volume numerical algorithm for thermoelastic phase-transition front propagation is described. A simple mathematical model of martensitic phase transition front propagation is considered. The phase transition front is viewed as an ideal mathematical discontinuity surface. The problem remains nonlinear even in this simplified description that requires a numerical solution. A non-equilibrium description of the process is provided by means of non-equilibrium jump relations at the moving phase boundary, which are formulated in terms of contact quantities. The same contact quantities are used in the construction of a finite-volume numerical scheme. The additional constitutive information is introduced by a certain assumption about the entropy production at the phase boundary. Results of numerical simulations show that the proposed approach allows us to capture experimental observations in agreement with theoretical predictions in spite of the idealization of the process.

Keywords: finite volume methods; martensitic phase transformations; moving phase boundary; thermomechanical modelling

1 Introduction

The propagation of waves and phase-transition fronts in thermoelastic media is governed by the same field equations and equations of state (at least in the

integral formulation). However, while these equations are sufficient for the description of thermoelastic waves, that is not the case for the phase transition fronts. It is well-known that initial-boundary-value problems, formulated according to the usual principles of continuum mechanics, can suffer from a lack of uniqueness of the solution when the body is composed of a multiphase material¹. The solution in this case involves a propagating phase boundary which separates the austenite from the martensite; the speed V_N of this interface remains undetermined by the usual continuum theory.

The propagation of phase interfaces in shape-memory alloys under applied stress is an experimentally observed phenomenon^{2,3}. It is also connected with a superelastic effect. Originally in the austenitic phase, martensite is formed, upon loading, beyond a certain stress level, resulting in the stress plateau shown in Fig. 1. The cause of stability of martensite at sufficiently high temperature is

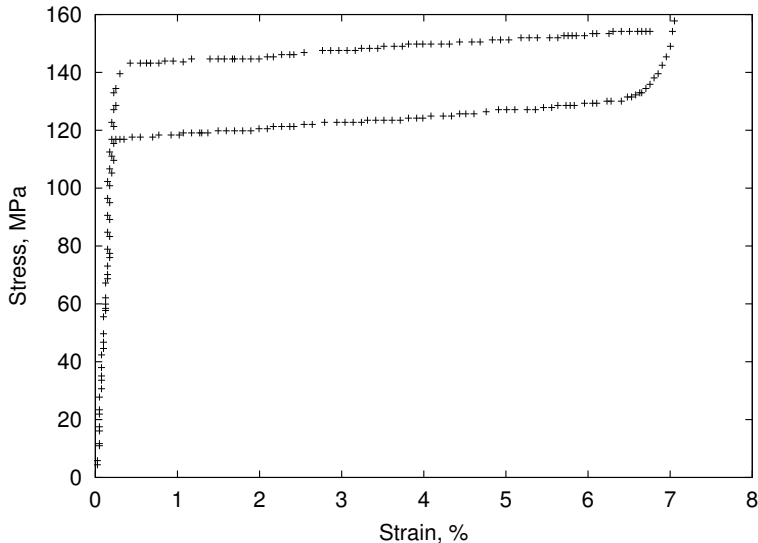


Figure 1: Experimental stress-strain relation for Cu-Zn-Al shape-memory alloy (from⁴).

the applied stress, and therefore upon unloading martensite becomes unstable and reverts to its parent phase gaining its undeformed shape. This effect, which causes the material to be extremely elastic, is known as pseudoelasticity or superelasticity. Therefore, the propagation of phase interfaces results in a non-classical nonlinear behavior of shape-memory alloys.

The simplest possible formulation of the stress-induced phase transition front propagation problem is given by Abeyaratne and Knowles⁵ in the case of an isothermal uniaxial motion of a slab in small-strain approximation. The phase front is represented by a jump discontinuity separating the different austenite and martensite branches of the N-shaped local stress-strain curve. A shift of the martensitic branch of the curve is provided by the incorporation of a trans-

formation strain, which is considered as an experimentally determined material constant.

From a thermodynamic point of view, a phase transition is a non-equilibrium process; entropy is produced at the moving phase boundary at a rate $f_S V_N$ ⁶. The entity f_S is called the driving force and may be expressed in terms of the limiting stress, deformation gradient and free-energy on the two sides of the interface^{1,5-8}. The uniqueness of the solution is provided by the introduction of two additional constitutive relations: a kinetic law for a driving force that establishes the speed of the transformation front

$$V_N = \phi(f_S), \quad (1)$$

where a constitutive function ϕ provides the continuum theory with a suitable description of the lattice transformation mechanism, and a nucleation criterion^{1,6,9}.

The prescription of the kinetic relation, of the nucleation criterion, and of the transformation strain means that the material behavior is completely known, and the numerical simulation is needed only for adjusting the values of coefficients of the model. In the considered model, the local equilibrium approximation is exploited in spite of the irreversibility of the phase transformation process. Moreover, to perform simulations of practical examples we need to move to a numerical approximation. In this case, we face a non-equilibrium behavior of finite-size discrete elements or computational cells. It is clear that the local equilibrium approximation is not sufficient to describe such a behavior.

Therefore a non-equilibrium description of the stress-induced phase-transition front propagation is preferable. To do this we need to choose an appropriate non-equilibrium theory. Our choice is influenced by numerical aspects of the modelling. This means that we need to have not only the non-equilibrium description of states of (finite volume) computational elements, but also the description of their interactions. In our opinion, the best possibility is provided by the thermodynamics of discrete systems¹⁰. In this theory, in addition to usual local equilibrium quantities, so-called contact quantities are introduced to provide the description of interactions between the systems. Therefore, the thermodynamic state space is extended.

The next step is to establish the non-equilibrium jump conditions at the phase interface. Each model of the stress-induced martensitic phase-transition front propagation uses its own jump relations¹¹⁻¹⁵. All of them differ from the classical equilibrium jump relations, which consist in the case of thermoelastic solids in the continuity of temperature and chemical potential and the continuity of the normal Cauchy traction at the phase boundary^{16,17}.

We apply the non-equilibrium jump relations¹⁸, which should be fulfilled for each pair of adjacent discrete elements. Supplementary constitutive information is introduced by means of certain assumptions about the entropy production at the phase boundary.

In order to include the non-equilibrium jump relations in the simulation, we apply a procedure which is similar to that proposed in¹⁹, but with a completely different numerical algorithm, based on the wave-propagation method

^{20,21}. However, we have made certain essential improvements to be able to apply it in the case of moving phase boundaries, e.g. In effect, we reformulate the algorithm in terms of contact quantities and non-equilibrium jump relations. The non-equilibrium jump relations are different for processes with and without entropy production ^{22,23}. This gives us the possibility to apply distinct non-equilibrium jump relations in the bulk (for the wave propagation without the entropy production) and at the phase boundary (where entropy is produced, since the phase transition is dissipative). The latter plays the role of a kinetic relation without an explicit specification. A thermodynamic criterion of initiation of the phase transition process follows from the simultaneous satisfaction of both distinct non-equilibrium jump relations at the phase boundary.

The chapter is organized as follows. The governing equations and jump relations for the simplest problem of a uniaxial phase transition front propagation in a slab are given in the Section 2. A discrete representation of the formulated problem is presented in the Section 3. Non-equilibrium jump relations at the phase boundary are introduced in the Section 4. The finite volume numerical scheme is discussed in the Section 5. The algorithm is presented in terms of contact quantities. We describe in detail how the contact quantities can be computed in the bulk and at the phase boundary. Results of numerical simulations and a comparison with available experimental data are given in the Section 6. Finally, main conclusions are presented in the Section 7.

2 Simple example: uniaxial motion of a slab

In order to explain some of the key ideas with a minimal mathematical complexity, it is convenient to work in an essentially one-dimensional setting. Following Abeyaratne and Knowles ⁵, we consider a slab, which in an unstressed reference configuration occupies the region $0 < x_1 < L$, $-\infty < x_2, x_3 < \infty$, and assume an uniaxial motion of the form

$$u_i = u_i(x, t), \quad x = x_1, \quad (2)$$

where t is time, x_i are the spatial coordinates, u_i are the components of the displacement vector. In this case, we have only three non-vanishing components of the strain tensor

$$\varepsilon_{11} = \frac{\partial u_1}{\partial x}, \quad \varepsilon_{12} = \varepsilon_{21} = \frac{1}{2} \frac{\partial u_2}{\partial x}, \quad \varepsilon_{13} = \varepsilon_{31} = \frac{1}{2} \frac{\partial u_3}{\partial x}. \quad (3)$$

Particle velocities associated with Eq. (2) are

$$v_i(x, t) = \frac{\partial u_i}{\partial t}. \quad (4)$$

Without loss of generality, we can set $\varepsilon_{13} = 0$, $v_3 = 0$ because of zero initial and boundary conditions for these components. Then we obtain uncoupled systems of equations for longitudinal and shear components which express the

balance of linear momentum and the time derivative of the Duhamel-Neumann thermoelastic constitutive equation, respectively, ^{22,23}:

$$\frac{\partial(\rho_0(x)v_1)}{\partial t} - \frac{\partial\sigma_{11}}{\partial x} = 0, \quad \frac{\partial}{\partial t} \left(\frac{\sigma_{11}}{\lambda(x) + 2\mu(x)} \right) - \frac{\partial v_1}{\partial x} = m(x) \frac{\partial\theta}{\partial t}, \quad (5)$$

and

$$\frac{\partial(\rho_0(x)v_2)}{\partial t} - \frac{\partial\sigma_{12}}{\partial x} = 0, \quad \frac{\partial}{\partial t} \left(\frac{\sigma_{12}}{\mu(x)} \right) - \frac{\partial v_2}{\partial x} = 0, \quad (6)$$

which are complemented by the heat conduction equation

$$C(x) \frac{\partial\theta}{\partial t} = \frac{\partial}{\partial x} \left(k(x) \frac{\partial\theta}{\partial x} \right). \quad (7)$$

Here σ_{ij} is the Cauchy stress tensor, ρ_0 is the density, θ is temperature, and C is the heat capacity per unit volume for a fixed deformation. The *dilatation coefficient* α is related to the thermoelastic coefficient m , and the Lamé coefficients λ and μ by $m = -\alpha(3\lambda + 2\mu)$. The indicated explicit dependence on the point x implies that the body is materially inhomogeneous in general.

The above description is well-known and these systems of equations can be solved separately. We focus our attention on the system of equations for shear components (Eq. 6) because the martensitic phase transformation is expected to be induced by shear.

2.1 Jump relations

To consider the possible irreversible transformation of a phase into another one, the separation between the two phases is idealized as a sharp, discontinuity surface \mathcal{S} across which most of the fields undergo finite jumps. Let $[A]$ and $\langle A \rangle$ denote the jump and mean value of a discontinuous field A across \mathcal{S} , the unit normal to \mathcal{S} being oriented from the “minus” to the “plus” side:

$$[A] := A^+ - A^-, \quad \langle A \rangle := \frac{1}{2}(A^+ + A^-). \quad (8)$$

Let $\tilde{\mathbf{V}}$ be the material velocity of the geometrical points of \mathcal{S} . The material velocity \mathbf{V} is defined by means of the inverse mapping $X = \chi^{-1}(x, t)$, where X denotes the material points ²⁴

$$\mathbf{V} := \left. \frac{\partial\chi^{-1}}{\partial t} \right|_x. \quad (9)$$

The phase transition fronts considered are *homothermal* (no jump in temperature; the two phases coexist at the same temperature) and *coherent* (they present no defects such as dislocations). Consequently, we have the following continuity conditions ^{25,26}:

$$[\mathbf{V}] = 0, \quad [\theta] = 0 \quad \text{at } \mathcal{S}. \quad (10)$$

Jump relations associated with the conservation laws in the bulk are formulated according to the theory of *weak solutions* of hyperbolic systems. Thus the jump relations associated with the balance of linear momentum and balance of entropy read ^{25,26}

$$\tilde{V}_N[\rho_0 v_2] + [\sigma_{12}] = 0, \quad \tilde{V}_N[S] + \left[\frac{k}{\theta} \frac{\partial \theta}{\partial x} \right] = \sigma_s \geq 0, \quad (11)$$

where S is entropy, \tilde{V}_N is the normal component of the material velocity of the points of \mathcal{S} , and σ_s is the entropy production at the interface. As shown in ^{25,26}, the entropy production can be expressed in terms of the driving force f_s such that the dissipation at the interface reads

$$f_s \tilde{V}_N = \theta_s \sigma_s \geq 0, \quad (12)$$

where θ_s is the temperature at \mathcal{S} . In addition, the *balance of material forces* at the interface between phases is found in the form ^{25,26}

$$f_s = -[W] + \langle \sigma_{ij} \rangle [\varepsilon_{ij}], \quad (13)$$

where W is the free energy per unit volume.

2.2 Dynamic loading

In a dynamic problem we look for piecewise smooth velocity and stress fields $v_2(x, t)$, $\sigma_{12}(x, t)$ for inhomogeneous thermoelastic materials, which obey the following initial and boundary conditions:

$$\sigma_{12}(x, 0) = v_2(x, 0) = 0, \quad \text{for } 0 < x < L, \quad (14)$$

$$v_2(0, t) = v_0(t), \quad \sigma_{12}(L, t) = 0, \quad \text{for } t > 0, \quad (15)$$

and satisfy the following field equations

$$\frac{\partial(\rho_0(x)v_2)}{\partial t} - \frac{\partial\sigma_{12}}{\partial x} = 0, \quad \frac{\partial}{\partial t} \left(\frac{\sigma_{12}}{\mu(x)} \right) - \frac{\partial v_2}{\partial x} = 0, \quad (16)$$

and jump conditions

$$\tilde{V}_N[\rho_0 v_2] + [\sigma_{12}] = 0, \quad [\mathbf{V}] = 0, \quad [\theta] = 0 \quad \text{at } \mathcal{S}, \quad (17)$$

$$f_s = -[W] + \langle \sigma_{ij} \rangle [\varepsilon_{ij}], \quad f_s \tilde{V}_N \geq 0. \quad (18)$$

It should be noted that Eqs. (17) and (18) are useless unless we could determine the value of the velocity of the phase boundary. A possible solution is the introduction of an additional constitutive relation between the material velocity at the interface and the driving force in the form of a kinetic relation ^{1,6,9}. Since the nonlinearity of the formulated problem due to the moving phase boundary requires a numerical solution, we postpone the introduction of the supplementary constitutive information to the numerical approximation.

3 Discrete representation

3.1 Integral balance laws for discrete elements

Following the main ideas of finite volume numerical methods ²¹, we divide the body in a *finite number of identical elements* of elementary volume Δx . Integration over the finite volume element of Eq. (16) yields the following set of integral forms:

$$\frac{\partial}{\partial t} \int_{\Delta x} \rho_0 v_2 dx = (\sigma_{12})^{right} - (\sigma_{12})^{left}, \quad (19)$$

$$\frac{\partial}{\partial t} \int_{\Delta x} \sigma_{12} dx = (\mu v_2)^{right} - (\mu v_2)^{left}. \quad (20)$$

3.2 Averaged quantities and fluxes

Introducing averaged quantities at each time step

$$\bar{v}_2 = \frac{1}{\Delta x} \int_{\Delta x} v_2 dx, \quad \bar{\sigma}_{12} = \frac{1}{\Delta x} \int_{\Delta x} \sigma_{12} dx, \quad (21)$$

and numerical fluxes at the boundaries of each element

$$F \approx \frac{1}{\Delta t} \int_{t_l}^{t_{l+1}} \sigma_{12} dt, \quad G \approx \frac{1}{\Delta t} \int_{t_l}^{t_{l+1}} \mu v_2 dt, \quad (22)$$

we are able to write a finite-volume numerical scheme for Eqs. (19), (20) for a uniform grid (n) in the form (l denotes time steps)

$$(\bar{v}_2)_n^{l+1} - (\bar{v}_2)_n^l = \frac{\Delta t}{\rho_n \Delta x} ((F^{right})_n^l - (F^{left})_n^l), \quad (23)$$

$$(\bar{\sigma}_{12})_n^{l+1} - (\bar{\sigma}_{12})_n^l = \frac{\Delta t}{\Delta x} ((G^{right})_n^l - (G^{left})_n^l). \quad (24)$$

The main difficulty in the construction of a numerical scheme is the proper determination of the numerical fluxes F, G ²¹. In fact our discrete elements are not in equilibrium, especially in the presence of phase transformation. Even if we can associate the averaged quantities with local equilibrium parameters, we still need to have a description of the non-equilibrium states of discrete elements. Moreover, we need also a description of interaction between these non-equilibrium elements, because classical equilibrium conditions are not valid in the case of fast propagation of sharp phase interfaces through the material during a stress-induced martensitic phase transformation.

4 Non-equilibrium jump conditions at the phase boundary

We start with the classical equilibrium conditions at the phase boundary. The classical equilibrium conditions at the phase boundary consist, for single-com-

ponent fluid-like systems, in the equality of temperatures, pressures and chemical potentials in the two phases, that is

$$[\theta] = 0 \quad \text{or} \quad \left[\left(\frac{\partial U}{\partial S} \right)_{V,M} \right] = 0, \quad (25)$$

$$[p] = 0 \quad \text{or} \quad \left[\left(\frac{\partial U}{\partial V} \right)_{S,M} \right] = 0, \quad (26)$$

$$[\mu] = 0 \quad \text{or} \quad \left[\left(\frac{\partial U}{\partial M} \right)_{S,V} \right] = 0, \quad (27)$$

where U is the internal energy, M is mass, V is volume, p is pressure, and μ is the chemical potential.

In the considered homothermal case, the continuity of temperature at the phase boundary still holds, and the continuity of the chemical potential can be replaced by the expression for the non-zero driving force (Eq. 18). What we need is to change the equilibrium condition for pressure (Eq. 26). In non-equilibrium, we expect that the value of internal energy of an element differs from its equilibrium value ²⁷

$$U = U_{eq} + U_{ex}, \quad (28)$$

where the excess energy U_{ex} is difference between the non-equilibrium and equilibrium values. Therefore, we can make a direct generalization of classical equilibrium condition for pressure using the excess energy

$$\left[\left(\frac{\partial(U_{eq} + U_{ex})}{\partial V} \right)_{S,M} \right] = 0. \quad (29)$$

However, the obtained jump relation corresponds to a fixed entropy at the boundary. At the same time, it is well understood that the martensitic phase transformation is a dissipative process, which involves entropy change. Therefore, we propose to replace the jump relation (Eq. 29) by another non-equilibrium jump relation. Our choice of the fixed variables is influenced by the stability conditions for single-component fluid-like systems ²⁸

$$\left[\left(\frac{\partial(U_{eq} + U_{ex})}{\partial V} \right)_{\theta,M} \right] = 0, \quad \left[\left(\frac{\partial(U_{eq} + U_{ex})}{\partial V} \right)_{p,M} \right] = 0. \quad (30)$$

The last two jump relations differ from Eq. (29) only by fixing different variables in the corresponding thermodynamic derivatives.

To be able to exploit the jump relations, we need to have a more detailed description of non-equilibrium states than by only introducing the energy excess. The most convenient description of the non-equilibrium states may be obtained by means of the thermodynamics of discrete systems ¹⁰, where the thermodynamic state space is extended by means of so-called *contact quantities*.

4.1 Contact quantities

We still deal with single-component fluid-like systems. A *discrete system*¹⁰ is considered as a domain separated from its equilibrium environment by a contact surface. In a Schottky system *per se*, the interaction between the system and the environment consists of heat, work and mass exchanges. These exchange quantities allow us to define so-called *contact quantities*. For instance, considering the heat exchange \dot{Q} , the *contact temperature*, Θ , is defined by the inequality¹⁰:

$$\dot{Q} \left(\frac{1}{\Theta} - \frac{1}{T^*} \right) \geq 0 \quad (31)$$

for vanishing work and mass exchange rates. Here T^* is the thermostatic temperature of the equilibrium environment. From Eq. (31) it follows that \dot{Q} and the bracket have always the same sign. We now suppose that there exists exactly one equilibrium environment for each arbitrary discrete system for which the net heat exchange between them vanishes. Then Eq. (31) determines the contact temperature Θ of the system as the thermostatic temperature T^* of the system's environment for which this net exchange vanishes. The *dynamic pressure*, p and *chemical potential*, μ are defined analogously¹⁰:

$$\dot{V} (p - p^*) \geq 0, \quad \dot{M} (\mu^* - \mu) \geq 0, \quad (32)$$

where \dot{V} is the time rate of volume, and \dot{M} is the time rate of mass.

The contact quantities so defined together with common local equilibrium variables provide a complete thermodynamic description of non-equilibrium states of a separated discrete system.

In the required extension to the *thermoelastic case*, the state of each element is identified with the thermodynamic state of a discrete system associated with it, each element being assumed in local equilibrium. In thermoelasticity, in addition to Θ and Eq. (31), which governs heat exchange, we must define a *contact dynamic stress tensor* Σ_{ij} . Analogously to Eq. (31) that holds for $\dot{\varepsilon}_{ij} = 0$ we have

$$\frac{\partial \varepsilon_{ij}}{\partial t} (\Sigma_{ij} - \sigma_{ij}^*) \geq 0, \quad (33)$$

for vanishing heat and mass exchange rates. Here σ_{ij}^* is the Cauchy stress tensor in the environment.

In the thermoelastic case, the thermodynamic derivatives which we should exploit instead of $\left(\frac{\partial U}{\partial V}\right)_\theta$ and $\left(\frac{\partial U}{\partial V}\right)_p$ are²⁸:

$$\left(\frac{\partial \bar{E}}{\partial \varepsilon_{ij}}\right)_\theta = -\bar{\theta} \left(\frac{\partial \bar{\sigma}_{ij}}{\partial \theta}\right)_\varepsilon + \bar{\sigma}_{ij}, \quad \left(\frac{\partial \bar{E}}{\partial \varepsilon_{ij}}\right)_\sigma = \bar{\theta} \left(\frac{\partial \bar{S}}{\partial \varepsilon_{ij}}\right)_\sigma + \bar{\sigma}_{ij}, \quad (34)$$

where E is the internal energy per unit volume and overbars denote the local equilibrium values.

Contact quantities are assumed to be connected with the excess energy in a similar way

$$\left(\frac{\partial E_{ex}}{\partial \varepsilon_{ij}}\right)_\theta = -\Theta \left(\frac{\partial \Sigma_{ij}}{\partial \theta}\right)_\varepsilon + \Sigma_{ij}, \quad \left(\frac{\partial E_{ex}}{\partial \varepsilon_{ij}}\right)_\sigma = \Theta \left(\frac{\partial S_{ex}}{\partial \varepsilon_{ij}}\right)_\sigma + \Sigma_{ij}, \quad (35)$$

where the interaction entropy S_{ex} is still undetermined. Using Eqs. (34), (35) we obtain from Eq. (30) that the parameters of the adjacent non-equilibrium elements of a thermoelastic continuum should satisfy the thermodynamic consistency conditions, the first of which is valid for all processes with no entropy production

$$\left[-\bar{\theta} \left(\frac{\partial \bar{\sigma}_{ij}}{\partial \theta} \right)_{\varepsilon} + \bar{\sigma}_{ij} - \Theta \left(\frac{\partial \Sigma_{ij}}{\partial \theta} \right)_{\varepsilon} + \Sigma_{ij} \right] \cdot N_j = 0, \quad (36)$$

and the second one corresponds to any inhomogeneity accompanied by entropy production

$$\left[\bar{\theta} \left(\frac{\partial \bar{S}}{\partial \varepsilon_{ij}} \right)_{\sigma} + \bar{\sigma}_{ij} + \Theta \left(\frac{\partial S_{ex}}{\partial \varepsilon_{ij}} \right)_{\sigma} + \Sigma_{ij} \right] \cdot N_j = 0. \quad (37)$$

Here N_j are components of the unit normal at the boundary of a discrete element. Now we are able to describe the non-equilibrium states of discrete elements and to exploit the non-equilibrium jump relations, if we can determine the values of contact quantities, which can be done at least numerically.

5 Finite-volume numerical scheme

5.1 Contact quantities in the bulk

We need now to solve the system of equations (Eq. 16). First we apply Eq. (36) to determine the values of the contact quantities in the absence of phase transformation. Since shear components of the stress tensor are independent of temperature, Eq. (36) reduces to

$$[\bar{\sigma}_{12} + \Sigma_{12}] = 0. \quad (38)$$

In the uniaxial case we have at the interface between elements $(n-1)$ and (n)

$$(\Sigma_{12}^+)_{n-1} - (\Sigma_{12}^-)_n = (\bar{\sigma}_{12})_n - (\bar{\sigma}_{12})_{n-1}. \quad (39)$$

This relation should be complemented by the kinematic condition between material and physical velocity²⁴, which in the small-strain approximation become

$$[\mathbf{v} + \mathbf{V}] = 0. \quad (40)$$

Assuming that the jump of the contact velocity is determined by the second term of Eq. (40)

$$[\mathcal{V}] = [\mathbf{V}], \quad (41)$$

we obtain in the uniaxial case

$$(\mathcal{V}_2^+)_{n-1} - (\mathcal{V}_2^-)_n = (\bar{v}_2)_n - (\bar{v}_2)_{n-1}. \quad (42)$$

At this step we need to introduce constitutive relations between contact stresses and contact velocities. Our choice is motivated by the possible reduction to the

wave-propagation algorithm. In fact, introducing the relations between contact stresses and contact velocities

$$(\mathcal{V}_2^-)_n = -\frac{(\Sigma_{12}^-)_n}{\rho_n c_n}, \quad (\mathcal{V}_2^+)_{n-1} = \frac{(\Sigma_{12}^+)_{n-1}}{\rho_{n-1} c_{n-1}}, \quad c = \sqrt{\frac{\mu}{\rho}}, \quad (43)$$

we obtain then a linear system of equations for the unknown contact velocities

$$(\mathcal{V}_2^+)_{n-1} - (\mathcal{V}_2^-)_n = (\bar{v}_2)_n - (\bar{v}_2)_{n-1}, \quad (44)$$

$$(\mathcal{V}_2^+)_{n-1} \rho_{n-1} c_{n-1} + (\mathcal{V}_2^-)_n \rho_n c_n = (\bar{\sigma}_{12})_n - (\bar{\sigma}_{12})_{n-1}. \quad (45)$$

The corresponding numerical scheme (23), (24) can be represented as

$$(\bar{\sigma}_{12})_n^{l+1} - (\bar{\sigma}_{12})_n^l = \frac{\Delta t}{\Delta x} \mu_n ((\mathcal{V}_2^+)_n^l - (\mathcal{V}_2^-)_n^l). \quad (46)$$

$$(\bar{v}_2)_n^{l+1} - (\bar{v}_2)_n^l = \frac{\Delta t}{\Delta x} \frac{1}{\rho_n} ((\Sigma_{12}^+)_n^l - (\Sigma_{12}^-)_n^l), \quad (47)$$

The two relations (Eqs. (44) and (45)) express together a characteristic property for the cell-centered numerical fluxes in the conservative wave-propagation algorithm²⁹, whose advantages we can therefore exploit. However, phase transitions are always accompanied by the production of entropy. Hence we need to apply another non-equilibrium jump relation at the phase boundary.

5.2 Contact quantities at the phase boundary

Suppose that the interface between two thermoelastic phases is placed between elements numbered $(p-1)$ and (p) . For the left element adjacent to the phase boundary, the contact quantities $(\Sigma_{12}^-)_{p-1}$ at the left boundary of the element can be determined within the above described numerical procedure. However, we need a more careful consideration for values of the contact stresses $(\Sigma_{12}^+)_{p-1}$ at the right side of the element which corresponds to the phase boundary. Similarly, for the right element adjacent to the phase boundary, we need to determine the values of $(\Sigma_{12}^-)_p$. The corresponding procedure is based on the non-equilibrium jump relation (Eq. 37) that is specified in the isothermal uniaxial case to be

$$\left[\bar{\theta} \left(\frac{\partial \bar{S}}{\partial \varepsilon_{12}} \right)_\sigma + \bar{\sigma}_{12} + \Sigma_{12} \right] = 0. \quad (48)$$

Here we should make certain assumption about the entropy production at the phase boundary. The simplest one is the continuity of contact stresses at the phase boundary

$$[\Sigma_{12}] = 0. \quad (49)$$

Another relation follows from the coherency conditions for the material velocity (Eq. 10) which can be expressed in the small-strain approximation as follows

$$[\mathcal{V}_2] = 0. \quad (50)$$

In terms of the contact stresses, the Eq. (50) yields

$$\frac{(\Sigma_{12}^+)_{p-1}}{\rho_{p-1}c_{p-1}} + \frac{(\Sigma_{12}^-)_p}{\rho_p c_p} = 0. \quad (51)$$

It follows from the Eqs. (49) and (51) that the values of contact stresses vanish at the phase boundary

$$(\Sigma_{12}^+)_{p-1} = (\Sigma_{12}^-)_p = 0. \quad (52)$$

Now all the contact quantities at the phase boundary are determined, and we can update the state of the elements adjacent to the phase boundary.

The material velocity at the interface is determined by means of the jump relation for linear momentum (Eq. 17)₁

$$V_N^2 = \frac{[\bar{\sigma}_{12}]}{\langle \rho_0 \rangle [\bar{\varepsilon}_{12}]}, \quad (53)$$

The direction of the front propagation is determined by the positivity of the entropy production (Eq. 12)

$$\sigma_s = \frac{f_s V_N}{\theta_s} \geq 0. \quad (54)$$

The obtained relations at the phase boundary are used in the described numerical scheme for the simulation of phase-transition front propagation.

6 Numerical simulations

6.1 Interaction of a plane wave with phase boundary

As a first example, we consider the interaction of a plane wave with a phase boundary to confirm the results of phase-transition front propagation in the one-dimensional case^{30–32}. The geometry of the problem is shown in Fig. 2. The wave is excited at the left boundary of the computation domain by prescribing a time variation of a component of the stress tensor. Upper and bottom boundaries are stress-free, the right boundary is assumed to be rigid. The time-history of loading is shown in Fig. 3. If the magnitude of the wave is high enough, the phase transformation process is activated at the phase boundary. The maximal value of the Gaussian pulse is chosen as 0.7 GPa. Material properties correspond to Cu-14.44Al-4.19Ni shape-memory alloy³³ in austenitic phase: the density $\rho = 7100 \text{ kg/m}^3$, the elastic modulus $E = 120 \text{ GPa}$, the shear wave velocity $c_s = 1187 \text{ m/s}$, the dilatation coefficient $\alpha = 6.75 \cdot 10^{-6} \text{ 1/K}$.

It was recently reported³⁴ that elastic properties of martensitic phase of Cu-Al-Ni shape-memory alloy after impact loading are very sensitive to the amplitude of loading. Therefore, for the martensitic phase we choose, respectively, $E = 60 \text{ GPa}$, $c_s = 1055 \text{ m/s}$, with the same density and dilatation coefficient as above. As a first result, the stress-strain relation is plotted in Fig. 4 at a

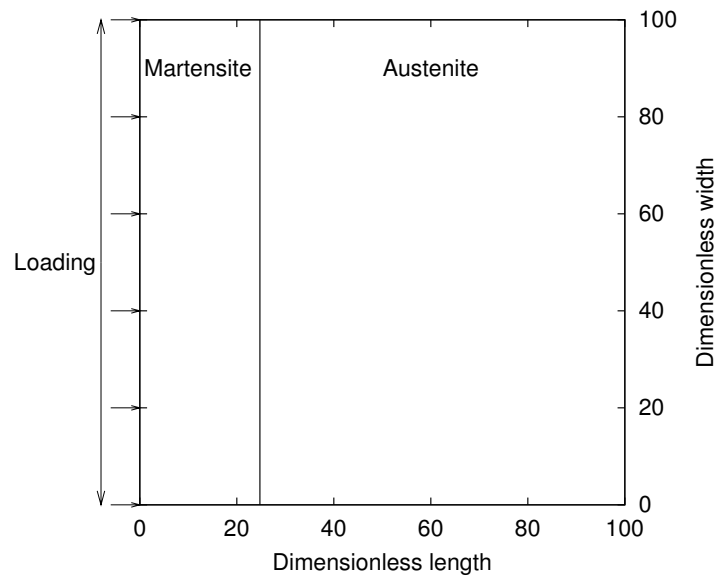


Figure 2: Plane wave: geometry.

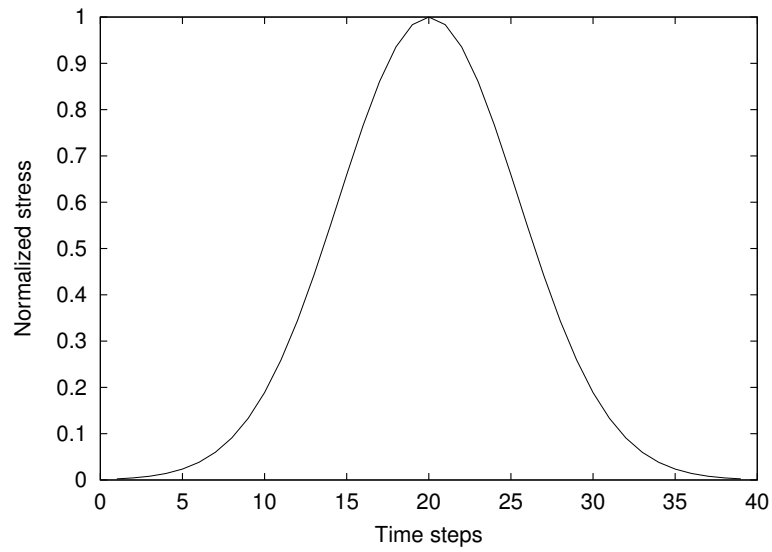


Figure 3: Loading time-history.

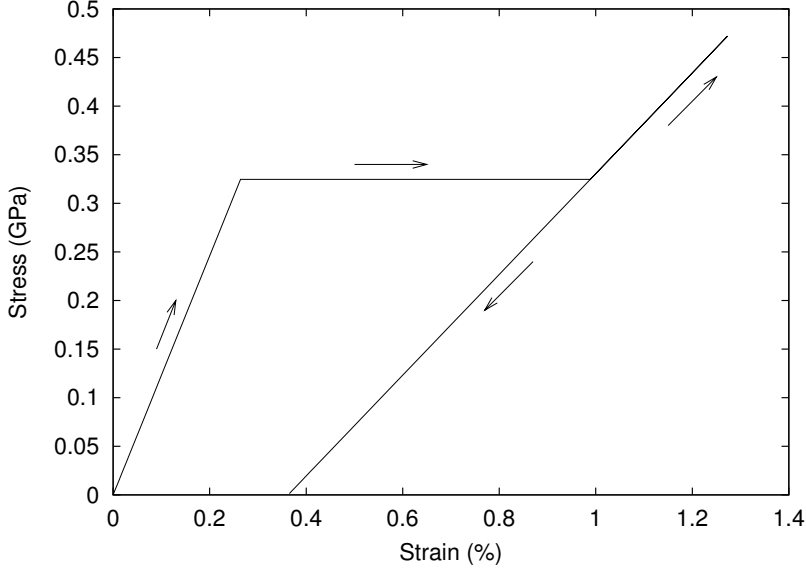


Figure 4: Stress-strain behavior at a fixed point if the transformation strain is taken into account.

fixed point inside the computational domain which was initially in the austenitic state. As we can see in Fig. 4, the stress-strain relation is at first linear corresponding to elastic austenite. Then the strain value jumps along a constant stress line to its value in the martensitic state due to phase transformation. Afterwards both loading and unloading correspond to elastic martensite. The value of the strain jump between straight lines, the slope of which is prescribed by material properties of austenite and martensite, respectively, is determined by the value of stress, that conforms to the critical value of the driving force, in agreement with the barrier of potential that we have to overcome to go from one phase to the other. Therefore, the stress value corresponding to the critical value of the driving force can be associated with the transformation stress, and the value of the strain jump corresponds to the transformation strain. We should then take into account that martensite can exist only in the deformed state, i.e. the martensitic line should start from a non-zero value of the transformation strain. The result shown in the Fig. 4, looks very much like the stress-strain dependence given in ⁵.

The obtained stress-strain relation at any fixed point results in overall pseudoelastic response of a specimen. The overall stress-strain behavior can be compared with the dynamic experiment provided in ³⁴ after adjusting the applied pulse width and shape (see Fig. 5) with an excellent agreement in the phase transformation region.

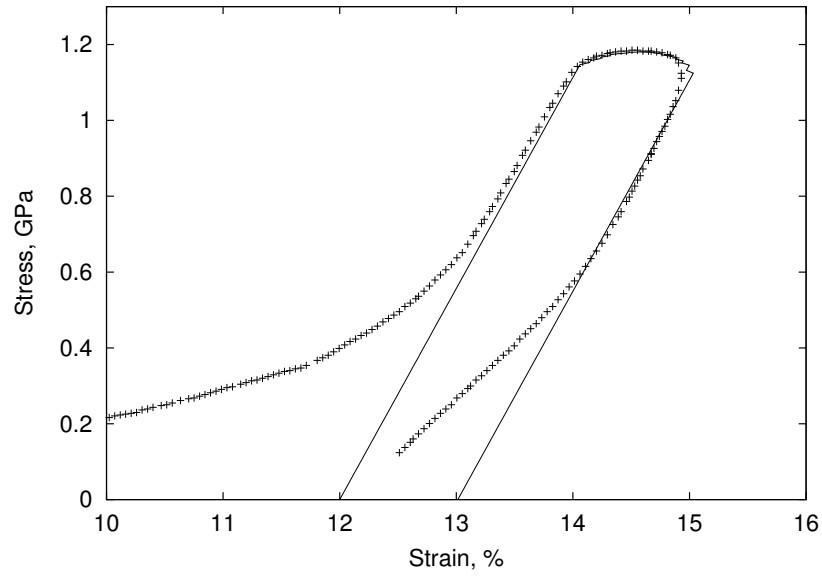


Figure 5: Stress-strain relation: comparison with experimental data from ³⁴ (sample 1).

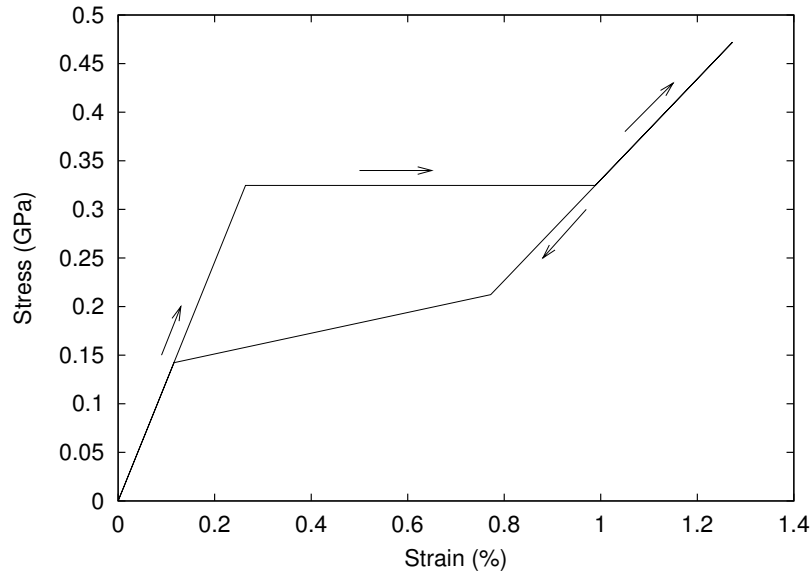


Figure 6: Stress-strain behavior at a fixed point with full recovering of austenite.

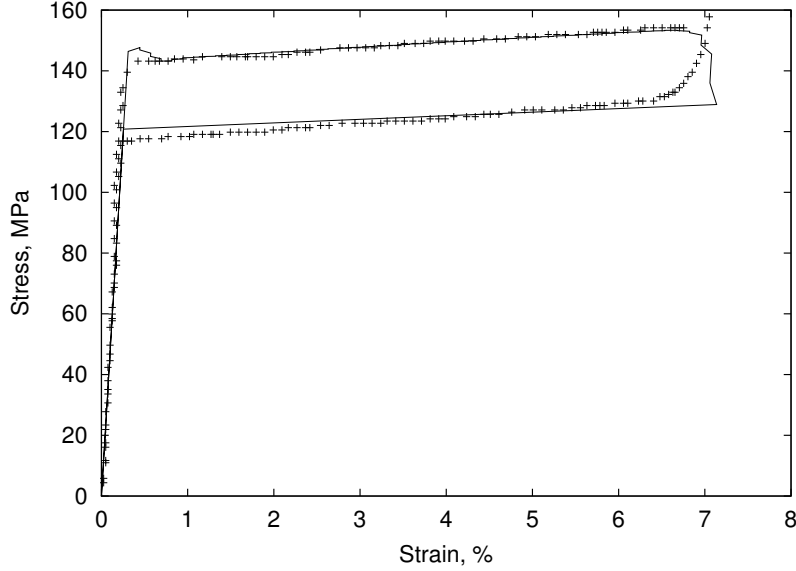


Figure 7: Stress-strain relation at the phase boundary: comparison with experimental data from ⁴.

6.2 Hysteretic behavior

Up to now it was supposed that austenite is not recovered after unloading which is not the case if the value of the reference temperature is above the onset of the reverse transformation temperature. The inverse phase transformation should occur immediately when the actual deformation of martensitic elements become less than the transformation strain. Since the inverse transformation is governed by another condition than the direct transformation, we obtain a hysteretic stress-strain behavior (Fig. 6). Again, the overall stress-strain dependence can be compared with experimental data. See Fig. 7, where the experimental data of a quasi-static loading of a similar material with relatively high applied loading rate (1 MPa/s) from ⁴ are given. The applied stress in this case was linearly increased and the duration of the impulse was chosen to fit the experimental data.

7 Conclusions

Attempts at numerical simulations of moving phase boundaries in solids meet the problems with constitutive modeling of the nucleation criterion and kinetic relation at the phase boundary, as well as with the construction of a proper numerical algorithm. In spite of the accuracy and stability of the wave propagation method for inhomogeneous media, its application to the phase-transition problems is impossible unless we can predict the values of numerical fluxes at the phase boundary. We have proposed to determine all the needed quanti-

ties by means of non-equilibrium jump relations at the phase boundary, which are presented by means of contact quantities derived from the thermodynamics of discrete systems. In this case the construction of the algorithm is complemented by the development of a thermodynamic model of phase-transition front propagation.

Results of numerical simulations show that the proposed approach allows us to reproduce experimental observations, in spite of the idealization of the process.

Acknowledgment

Support of the Estonian Science Foundation under contracts No. 4504, 5765 (A.B., J.E.), of the European Network TMR. 98-0229 on "Phase transitions in crystalline substances" (G.A.M.) and of ESF Scientific Programme on Nonlinear Acoustic Techniques for Micro-Scale Damaged Diagnostics (NATEMIS) (A.B., J.E.) is gratefully acknowledged. G.A.M. benefits from a Max Planck Award for International Cooperation (2001-2005). Research achieved within the Parrot French-Estonian Program (2003-2004).

References

- [1] R. Abeyaratne and J. K. Knowles, Kinetic relations and the propagation of phase boundaries in solids, *Arch. Rat. Mech. Anal.* **114**, 119–154 (1991).
- [2] J. A. Shaw and S. Kyriakides, Thermomechanical aspects of NiTi, *J. Mech. Phys. Solids* **43**, 1243–1281 (1995).
- [3] J. A. Shaw and S. Kyriakides, On the nucleation and propagation of phase transformation fronts in a NiTi alloy, *Acta Mater.* **45**, 673–700 (1997).
- [4] B. C. Goo and C. LExcellent, Micromechanics-based modeling of two-way memory effect of a single-crystalline shape-memory alloy, *Acta Mater.* **45**, 727–737 (1997).
- [5] R. Abeyaratne, K. Bhattacharya, and J. K. Knowles, Strain-energy functions with local minima: Modeling phase transformations using finite thermoelasticity, in: *Nonlinear Elasticity: Theory and Application*, edited by Y. Fu and R. W. Ogden (Cambridge University Press, Cambridge, 2001), pp. 433–490.
- [6] R. Abeyaratne and J. K. Knowles On the driving traction acting on a surface of strain discontinuity in a continuum, *J. Mech. Phys. Solids* **38**, 345–360 (1990).
- [7] L. Truskinovsky, Dynamics of nonequilibrium phase boundaries in a heat conducting nonlinear elastic medium, *J. Appl. Math. Mech. (PMM)* **51**, 777–784 (1987).

- [8] G. A. Maugin and C. Trimarco, The dynamics of configurational forces at phase-transition fronts, *Meccanica* **30**, 605–619 (1995).
- [9] J. K. Knowles, Stress-induced phase transitions in elastic solids, *Comp. Mech.* **22**, 429–436 (1999).
- [10] W. Muschik, Fundamentals of non-equilibrium thermodynamics, in: *Non-Equilibrium Thermodynamics with Application to Solids*, edited by W. Muschik (Springer, Wien, 1993), pp. 1–63.
- [11] Y. C. Chen and D. C. Lagoudas, Impact induced phase transformation in shape memory alloys, *J. Mech. Phys. Solids* **48**, 275–300 (2000).
- [12] A. Bekker, J. C. Jimenez-Victory, P. Popov, and D. C. Lagoudas, Impact induced propagation of phase transformation in a shape memory alloy rod, *Int. J. Plasticity* **18**, 1447–1479 (2002).
- [13] D. C. Lagoudas, K. Ravi-Chandar, K. Sarh, and P. Popov, Dynamic loading of polycrystalline shape memory alloy rods, *Mechanics of Materials* **35**, 689–716 (2003).
- [14] J. A. Shaw, A thermomechanical model for a 1-D shape memory alloy wire with propagating instabilities, *Int. J. Solids Struct.* **39**, 1275–1305 (2002).
- [15] V. Stoilov and A. Bhattacharyya, A theoretical framework of one-dimensional sharp phase fronts in shape memory alloys, *Acta Mater.* **50**, 4939–4952 (2002).
- [16] M. A. Grinfeld, *Thermodynamic Methods in the Theory of Heterogeneous Systems* (Longman, London, 1991).
- [17] P. Cermelli and S. Sellers, Multi-phase equilibrium of crystalline solids, *J. Mech. Phys. Solids* **48**, 765–796 (2000).
- [18] A. Berezovski and G. A. Maugin, On the thermodynamic conditions at moving phase-transition fronts in thermoelastic solids, *J. Non-Equilib. Thermodyn.* **29**, 37–51 (2004).
- [19] X. Zhong, T. Y. Hou, and P. G. LeFloch, Computational methods for propagating phase boundaries, *J. Comp. Physics* **124**, 192–216 (1996).
- [20] R. J. LeVeque, Wave propagation algorithms for multidimensional hyperbolic systems, *J. Comp. Physics* **131**, 327–353 (1997).
- [21] R. J. LeVeque, *Finite Volume Methods for Hyperbolic Problems* (Cambridge University Press, Cambridge, 2002).
- [22] A. Berezovski and G. A. Maugin, Simulation of thermoelastic wave propagation by means of a composite wave-propagation algorithm, *J. Comp. Physics* **168**, 249–264 (2001).

- [23] A. Berezovski, J. Engelbrecht, and G. A. Maugin, Thermoelastic wave propagation in inhomogeneous media, *Arch. Appl. Mech.* **70**, 694–706 (2000).
- [24] G. A. Maugin, *Material Inhomogeneities in Elasticity* (Chapman and Hall, London, 1993).
- [25] G. A. Maugin, Thermomechanics of inhomogeneous - heterogeneous systems: application to the irreversible progress of two- and three-dimensional defects, *ARI* **50**, 41–56 (1997).
- [26] G. A. Maugin, On shock waves and phase-transition fronts in continua, *ARI* **50**, 141–150 (1998).
- [27] W. Muschik and A. Berezovski, Thermodynamic interaction between two discrete systems in non-equilibrium, *J. Non-Equilib. Thermodyn.* **29**, 237–255 (2004).
- [28] H. B. Callen, *Thermodynamics* (Wiley & Sons, New York, 1960).
- [29] D. S. Bale, R. J. LeVeque, S. Mitran, and J. A. Rossmannith, A wave propagation method for conservation laws and balance laws with spatially varying flux functions, *SIAM J. Sci. Comp.* **24**, 955–978 (2003).
- [30] A. Berezovski and G. A. Maugin, Thermoelastic wave and front propagation, *J. Thermal Stresses* **25**, 719–743 (2002).
- [31] A. Berezovski and G. A. Maugin, Thermodynamics of discrete systems and martensitic phase transition simulation, *Technische Mechanik* **22**, 118–131 (2002).
- [32] A. Berezovski, J. Engelbrecht, and G. A. Maugin, A thermodynamic approach to modeling of stress-induced phase-transition front propagation in solids, in: *Mechanics of Martensitic Phase Transformation in Solids*, edited by Q. P. Sun (Kluwer, Dordrecht, 2002), pp. 19–26.
- [33] J. C. Escobar and R. J. Clifton, On pressure-shear plate impact for studying the kinetics of stress-induced phase-transformations, *Mat. Sci. & Engng.* **A170**, 125–142 (1993).
- [34] Y. Emel'yanov, S. Golyandin, N. P. Kobelev, S. Kustov, S. Nikanorov, G. Pugachev, K. Sapozhnikov, A. Sinani, Ya. M. Soifer, J. Van Humbeeck, and R. De Batist, Detection of shock-wave-induced internal stresses in Cu-Al-Ni shape memory alloy by means of acoustic technique, *Scripta mater.* **43**, 1051–1057 (2000).